Effect of the Nature of the Counterion on the Properties of Anionic Surfactants. 4. Characterizing Micelles of Tetraalkylammonium Dodecyl Sulfate as Reaction Media

Barney L. Bales,*,† Mohamed Benrraou,‡ Kaba Tiguida,‡ and Raoul Zana‡

Department of Physics and Astronomy and the Center for Supramolecular Studies, California State University at Northridge, Northridge, California 91330-8268, and Institut C. Sadron (ICS-ULP), 6 rue Boussingault, 67000 Strasbourg, France

Received: November 22, 2004; In Final Form: January 27, 2005

Micelles formed in water from tetramethyl-, tetraethyl-, tetrapropyl- and tetrabutylammonium dodecyl sulfate (TMADS, TEADS, TPADS, and TBADS, respectively) are characterized as reaction media. All of the results are identical in the presence or absence of added salt, provided micelles of the same aggregation number, *N*, are compared. The microviscosity (η) deduced from the rotational motion of the nitroxide group of a spin probe increases modestly as a function of *N* in TMADS and TEADS, decreases slightly in TPADS, and decreases slightly before increasing in TBADS. The activation energy for the viscosity is remarkably similar in all of the tetraalkylammonium dodecyl sulfate (TAADS) micelles and is similar to that in ethanol/water mixtures as well as other anionic and cationic micelles. The volume fraction occupied by water in the polar shell, $H(t)$, decreases with *N* in TMADS, TEADS, and TPADS at 10, 25, and 45 °C whereas it decreases, goes through a minimum, and then increases in TBADS. $H(t)$ also decreases with the size of the counterion. The bimolecular collision rate as deduced from fluorescence quenching of pyrene by dodecylpyridinium chloride conforms well to a hydrodynamic description, varying linearly with T/η, where *T* is the absolute temperature and passing through the origin. Quenching probablities of 0.53, 0.51, 0.45, 0.39 for TMADS, TEADS, TPADS, and TBADS, respectively, are rationalized in terms of small shifts of the diffusion zones outside of the Stern layer by an average of 16% of the Stern layer thickness.

Introduction

This paper is a continuation of a series[1−3] in which we are investigating the effect of rather large, somewhat hydrophobic tetraalkylammonium counterions on the properties of anionic micelles. We shall refer to parts 1,[1] 2,[2] and 3[3] in this paper. In part 1,[1] the critical micelle concentrations in the absence of added salt (cmc_0), the ionization degree at the cmc_0 (α^0) deduced from conductivity measurements, and the aggregation numbers (*N*) were presented for tetramethyl-, tetraethyl-, tetrapropyl- and tetrabutylammonium dodecyl sulfate (TMADS, TEADS, TPADS, and TBADS, respectively). Part 2[2] detailed the determination of the ionization degree using a recently introduced hypothesis[4] that the aggregation number depends only on the concentration of counterions in the aqueous phase. Part 3[3] presented further values of *N* for TBADS and detailed two unusual features of this surfactant: (1) clouding and (2) aggregation numbers that increase as a function of temperature. Here, we continue a program to characterize micelles as variable reaction media (microreactors) that has thus far been applied to sodium dodecyl sulfate (SDS),[5,6] SDS mixed with heptane,[7] mixed micelles of SDS and a sugar-based nonionic surfactant,[8,9] and to the cationic micelles dodecyltrimethylammonium chloride (DTAC) and bromide (DTAB).[10] Specifically, this characterization consists of measuring the micelle ionization degree,[4] estimating the concentration of water in the Stern layer by a direct probe method,[5] measuring the microviscosity,[8,10] and rationalizing the bimolecular collision rate constant in terms of a hydrodynamic description.[8,10] The goal of such work is to be able to predict the micelle ionization degree, hydration, microviscosity, and bimolecular collision rates as a function of variable experimental parameters and thus be able to tailor a microreactor to the needs of an anticipated experiment. This work, which inserts bulky counterions into the Stern layer of dodecyl sulfate micelles, complements earlier work[8,9,11] that considered the effect of inserting a bulky sugar headgroup into SDS micelles. Like the earlier work,[8,9,11] we find that the bulky counterions expel water. In contrast, we find that inserting bulky counterions has practically no effect on the microviscosity whereas the headgroups had a profound effect.[8]

Methods

Experimental details for the electron paramagnetic resonance (EPR) measurements are identical to those described recently;[8] essential details are summarized. Mother solutions of the surfactants prepared at concentrations $C \approx 400$ mM containing the spin probe 16-doxylstearic acid methyl ester (16DSE) with a surfactant-to-probe ratio of 500:1 were prepared in MilliQ water. Solutions with various combinations of surfactant and salt were prepared from the mother solution by weight; their concentrations are presented assuming that the solution density is 1.0 g/cm^3. All EPR spectra in tetraalkylammonium dodecyl sulfate (TAADS) micelles consisted of three narrow lines typical of nitroxide spectra in the motional narrowing region. See Figure 1 of part 2[2] for typical spectra. Spectra in neat TBADS, a viscous ionic liquid,[3] showed effects of slower motion below 45 °C. Computer fits of the EPR spectra yield the line positions, shapes, and heights to high precision.[12]

* Corresponding author. E-mail: barney.bales@csun.edu. Web page: http://www.csun.edu/~vcphy00s/bales.html.
† California State University at Northridge.
‡ Institut C. Sadron.

10.1021/jp040728s CCC: $30.25 © 2005 American Chemical Society
Published on Web 03/30/2005

TABLE 1: Coefficients in Eq 2

t, °C	$A_+^{\text{eff}}(0)$, G	$(\partial A_+/\partial H)$, G
10	14.227 ± 0.007[a]	1.572 ± 0.013[a]
25	14.309[b]	1.418[b]
45	14.307 ± 0.007[a]	1.379 ± 0.012[a]

[a] Mean and standard deviation in two experiments. [b] Reference 11.

Rotational correlation times of the nitroxide group were computed from the line height ratios using standard formulas[13] and are corrected for inhomogeneous line broadening.[14] Two independent values of the rotational correlation time result,[13] τ_B and τ_C. Isotropic reorientation of the nitroxide moiety yields $\tau_B = \tau_C$, thus the departure of the ratio τ_B/τ_C from unity is a measure of the anisotropy of the motion of the nitroxide group.[15] The effective rotational correlation time is defined by[15]

$$\tau_{\text{measured}} = \sqrt{\tau_B \cdot \tau_C} \tag{1}$$

From the EPR line positions, the hyperfine spacing between the center- and low-field lines, A_+, is computed. Mukerjee et al.[16] introduced a nonempirical polarity scale, H(25 °C), which, for solvent mixtures with no other source of OH dipoles than water, is equal to the volume fraction occupied by water.[5] H(25 °C) and A_+ have been shown to be linearly correlated,[11,16] allowing the former to be deduced from the latter using calibration curves. In this work, we have found that H(25 °C) extends to values below those for which the previous calibration[11] of A_+ is valid, so a new calibration seemed necessary; however, as the Appendix details, no change at 25 °C proved to be necessary. We present data at temperatures other than 25 °C, so an extension of the calibration must be made to other temperatures. The details of this calibration are given in the Appendix, yielding

$$A_+^{\text{eff}} = A_+^{\text{eff}}(0) + \left(\frac{\partial A_+}{\partial H}\right) H(t) \tag{2}$$

where $H(t)$ is Mukerjee's hydrophilicity index[16] at temperature t (°C) and $A_+^{\text{eff}}(t) = A_+(t) - 0.0024(t - 25°)$ corrects the value of A_+ measured at t for the intrinsic variation of the hyperfine spacing with temperature. The parameters in eq 2 are given in Table 1.

See refs 5, 8, 11, 16−18 and references therein for a thorough discussion of the suitability of the use of the solvatochromic properties of nitroxide free radicals to study lipid assemblies such as micelles, the theoretical basis[17] for the variation of A_+ with $H(t)$, and the methods[5,11] to obtain calibration curves such as eq 2.

The results of this study are presented as functions of the aggregation number N. The ease of the EPR experiments permit much more extensive measurements than are feasible in experiments such as time-resolved fluorescence quenching (TRFQ)[1] and small-angle neutron scattering (SANS)[19] that yield experimental estimates of the values of N; thus, interpolation is necessary to present the EPR results. This is accomplished by exploiting the fact that for TMADS, TEADS, and TPADS, N varies with the concentration of counterions in the aqueous phase, C_{aq}, as follows:

$$N = N^0 (C_{aq}/\text{cmc}_0)^{\gamma} \tag{3}$$

where N^0 is the aggregation number at the cmc without added salt (cmc_0) and γ is a constant. For TBADS, at 25 °C, N varies linearly (see Figure 5b of ref 2) as follows:

TABLE 2: Parameters in Equation 3

	T, °C	cmc_0, mM[a]	α[b]	N^0 [b]	γ[b]
TMADS	10	5.4	0.32	74	0.10
TMADS	25	5.4	0.34	61	0.10
TMADS	45	5.7	0.37	53[c]	0.10
TEADS	25	3.7	0.44	62	0.05
TPADS	25	2.2	0.45	54	0.06

[a] Reference 1. [b] Reference 2. [c] Extrapolated from 40 °C.

$$N = 47 + 1.6(C_{aq}/\text{cmc}_0) \tag{4}$$

C_{aq} is given by

$$C_{aq} = \{\alpha C + (1 - \alpha) C_{\text{free}} + C_{ad}\}/(1 - VC) \tag{5}$$

where C is the total concentration of TAADS, C_{ad} is the concentration of added TAACl, V is the molar volume of TAADS assuming that the density of the anhydrous surfactant is 1.0 g/cm^3, and α is the micelle ionization degree. The parameters in eqs 3−5 are given in Table 2. C_{free} is the molar concentration of the surfactant in monomer form, which may be computed using eq 5 of ref 20 derived from the work of Sasaki et al.[21] and Hall,[22] as follows:

$$\log(C_{\text{free}}) = (2 - \alpha)\log(\text{cmc}_0) - (1 - \alpha)\log(C_{aq}) \tag{6}$$

At low values of C_{aq}, the values of C_{free} given by eq 6 are sensitive to the value of cmc_0 but are rather insensitive to the value of α.

Theory

Microviscosity from EPR Measurements of the Rotational Correlation Time. The microviscosity of the environment of a spin probe may be estimated utilizing the Debye−Stokes−Einstein equation[23]

$$\tau_{\text{relative}} = 4\pi\eta R_h^3/3kT \tag{7}$$

where η is the shear viscosity of the solvent, k is the Boltzmann constant, T is the absolute temperature, and R_h is the effective hydrodynamic radius of the nitroxide probe group, which was found[8] to be $R_h = 3.75$ Å for 16DSE. In micelles, the viscosity is replaced by the microviscosity. The subscript *relative* refers to reorientation of the nitroxide group relative to a liquid at rest. To estimate the microviscosity from rotational correlation times measured in the laboratory frame of reference, τ_{measured}, the overall motion of the doxyl group is modeled as a reorientation relative to the micelle as a unit with rotational correlation time τ_{relative} and an isotropic reorientation of the micelle as a whole with a characteristic time τ_{micelle}. These reorientations are assumed to be independent, so

$$\frac{1}{\tau_{\text{measured}}} = \frac{1}{\tau_{\text{relative}}} + \frac{1}{\tau_{\text{micelle}}} \tag{8}$$

τ_{micelle} is computed from the Debye−Stokes−Einstein equation written as follows:

$$\tau_{\text{micelle}} = V_{\text{micelle}} \cdot \frac{\eta_w}{kT} \tag{9}$$

where η_w is the viscosity of pure water[24] and $V_{micelle}$ is approximated by assuming the rotating micelle to be a sphere

$$V_{micelle} = \frac{4}{3}\pi R_m^3 \quad (10)$$

where R_m is the micelle radius found by adding the thickness of the Stern layer to the core radius given below in eq 14. Further details on applying eqs 7−10 may be found in ref 25.

Fluorescence Quenching in Dodecyl Sulfate Micelles. A hydrodynamic theory of the quenching rate constant between molecules in micelles was recently introduced[8] and expanded.[6] Combining the Smolukhovsky and the Stokes−Einstein equations yields the quenching rate constant

$$k_q = P\frac{8C_Q RT}{3000\eta} \quad (11)$$

where $R = 8.31$ J/K is the gas constant, T is the absolute temperature, C_Q is the concentration (ML^{-1}) of the quencher, and η has unit Poise. In this paper, we refer to eq 11 as the Stokes−Einstein−Smolukhovsky (SES) equation.

In bulk liquid, the factor, P, is interpreted to be the probability that the quenching of the excited state of the fluorophore occurs upon collision, C_Q is computed using the entire sample volume, and η is a constant throughout the sample. In a micelle, the situation is considerably more complicated;[6] nevertheless, despite some necessary simplifying assumptions, the SES has already met with success in the cases in which it has been tested.[6−8,10] The SES predicts that all molecules collide with the same rate constant in all solvents. This has been found to be approximately true in bulk solvent for several fluorophore-quenchers pairs; for example, pyrene-hexadecylpyridinium chloride (C_{16}PC; in general for n carbons, C_nPC) in methanol,[6] pyrene−C_{16}PC in water,[26] pyrene-5-doxylstearicacid methyl ester (5DSE) in methanol,[6] 1-methylpyrene−C_{14}PC in methanol, and pyrene−dimethylbenzophenone (DMBP) in methanol.[6] In all of these cases, P was found to be near unity. In micelles, the independence of the rate constant on the nature of the quencher has been confirmed, for example, for C_9PC, C_{10}PC, C_{12}PC in hexadecyltrimethylammonium chloride and acetate[27] and for C_{16}PC, DMBP, and 5DSE in SDS.[6] However, in micelles, P has been found to be less than unity.[6−8, 10]

A zero-order model of the application of eq 11 to micelles was introduced[6] previously and assumes the following:

1. A simple approximately spherical core−shell model[28] describes dodecyl sulfate micelles.

2. Fluorophores and all quenchers diffuse throughout the volume of the polar shell and nowhere else.

3. The spin probe diffuses throughout the volume of the polar shell and nowhere else and thus reports a viscosity, which is the average of the zone through which the fluorophore and the quenchers diffuse.

4. The probability of quenching upon collision between a given fluorophore-quencher pair is the same in bulk liquid and in a micelle.

The concentration C_Q in a micelle is computed over the volume through which the quencher diffuses. Because k_q is the quenching rate constant due to one quencher, then, assuming for simplicity that this concentration is constant throughout the diffusion volume and zero elsewhere, C_Q is the molar concentration of one molecule in the volume of the shell, V_{shell}, thus

$$C_Q = \frac{10^{27}}{N_0 V_{shell}} \quad (12)$$

where N_0 is Avogadro's number and V_{shell} is in units Å^3. The factor 10^{27} results from the conversion from Å^3 to liters.

V_{shell} is given by

$$V_{shell} = \frac{4\pi}{3}(R_m^3 - R_c^3) \quad (13)$$

The core radius is computed from

$$NV_{tail} = \frac{4\pi}{3}R_c^3 \quad (14)$$

where V_{tail} is the volume of one alkyl chain embedded in the core.[29] Assuming all 12 carbons to be within the core gives $V_{tail} = 350$ Å^3.[29] Assuming that some alkyl methylene or terminal methyl groups are located in the Stern layer changes the value of R_c; however, V_{shell} is rather insensitive to this change. The shell thickness dominates.

The zero-order model predicts that, in micelles, all quencher -fluorophore pairs would be consistent with eq 11 with P equal to its value in bulk liquids. Experimentally, it has been found that the SES describes the results rather well in that k_q varies nearly linearly with T/η and extrapolates reasonably to the origin as predicted; however, in every case studied thus far[6−8,10] and in the results to be presented in this work, P is less than unity. That this would be so is understandable because the zero-order model requires that both the fluorophore and the quencher diffuse through exactly the same volume, namely that of the polar shell. Because this is unlikely, a first-order correction was proposed,[6] which envisions that these volumes could be somewhat different.

If these volumes are different then the probability in eq 11 becomes the product of the probabilities that the two molecules collide and that quenching occurs upon collision. For simpicity, we set the quenching probability equal to unity for C_{12}PC. Therefore, in micelles the factor P in eq 11 becomes equal to the probability of collision. Below, we present a model to calculate this probability in dodecyl sulfate micelles.

Results

Hydration of Polar Shell. From the measured values of A_+, the polarity indices $H(t)$ were computed from eq 2. For TMADS, these are plotted versus the aggregation numbers, computed from eq 3, for $t = 10$, 25, and 45 °C in Figure 1. Each point is the mean value of five spectra collected one after the other; the standard deviations are about $^1/_{10}$th the size of the plot symbols. There were four runs using freshly prepared samples as detailed in the Supporting Information. Comparing the four runs at 25 °C showed that the reproducibility with samples presumably prepared in the same way was about the size of the symbols in Figure 1. The data from a typical run are shown in Figure 1 employing samples prepared using various combinations of surfactant and salt concentrations. The open points in Figures 1−3, 5, and 7 of this paper are derived from salt-free samples and the closed from salt-added samples. The results in Figure 1 show that volume fraction of water decreases with increasing aggregation number, which has been invariably found by EPR[5,10,18] and by chemical trapping.[30] Even the tetramethylammonium counterion (TMA^+) is already rather large compared with previously studied Na^+ and Li^+ in dodecyl sulfate[5,18] and Br^- and Cl^- in dodecyltrimethylammonium micelles.[10] Therefore, it is not straightforward to apply the simple geometric hydration models[5,8,10,11,18] developed in the past because the counterions have diameters near to or larger than the 5 Å thickness of the polar shell used in those models. This prevents

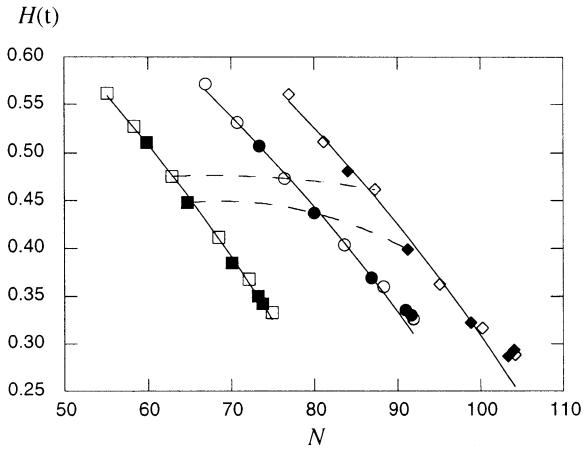

Figure 1. Volume fraction occupied by water vs the aggregation number for TMADS micelles at 10 °C (◆, ◇), 25 °C (●, ○), and 45 °C (■, □). Open symbols, no added TMACl; closed, added TMACl. Solid lines are from a two parameter fit not discussed and serve to guide the eye. The dashed lines trace the dependence of two of the samples on the temperature. Mean values of 5 measurements with standard deviations about 1/10 the size of the symbols.

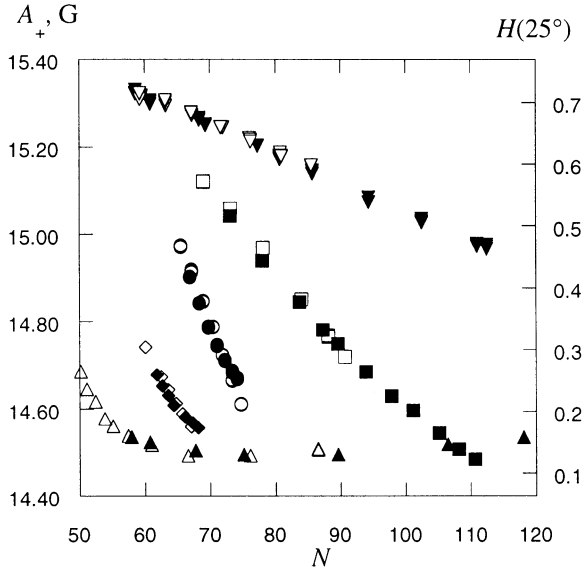

Figure 2. A_+ and the volume fraction occupied by water vs the aggregation number for SDS (▼, ▽),[12] TMADS (■, □), TEADS (●, ○), TPADS (◆, ◇), and TBADS (▲, △) micelles at 25 °C. Open symbols, no added TAACl; closed, added TAACl.

a quantitative comparison between theory and experiment in the manner that we have done in the past.[5] Despite this lack of detail, it is clear that the polar shell of the TAADS micelles becomes dryer as the counterion becomes larger. This is the anticipated result: the larger counterions displace more water leading to smaller values of H(25 °C) at a given value of N. A similar effect is observed when larger headgroups are placed into SDS micelles.[11]

The temperature dependence of the data in Figure 1 could be interpreted in at least two ways. Assuming that 16DSE maintains its average location as the temperature varies would mean that TMADS micelles become less hydrated at higher temperatures when micelles of the same value of N are compared. Figure 1 shows that the drying of the Stern layer with increasing N occurs at similar rates at all three temperatures. An alternate interpretation of the data is possible: that 16DSE changes average positions with temperature. This latter possibility may be tested by employing other spin probes. Very similar behavior with N and T as that in Figure 1 is observed in TEADS; three roughly parallel curves result (not shown).

Figure 2 displays values of the volume percentage occupied by water in TMADS, TEADS, TPADS, and TBADS micelles versus the aggregation numbers computed from eqs 3 and 4 at 25 °C as well as the same data for SDS taken from the literature.[12] In all cases, H(25 °C) decreases upon increasing N as has invariably been found to be the case; however, for TBADS, a minimum occurs followed by a subsequent slight *increase* in hydration. The volume percentage of water decreases as a function of the size of the counterion, as expected, producing reaction media that are rather dry in all of the TAADS micelles as the aggregation numbers increase. The hydration of these micelles depends only on their aggregation numbers, regardless of whether salt is added or not. The absolute values of H(25 °C) in Figure 2 are thought to be rather accurate for H(25 °C) > 0.3; however, at lower values, polarization effects could become important, introducing errors.[31] The relative values H(25 °C) are likely to be accurate.

In dodecyl sulfate micelles involving inorganic counterions (Na^+ or Li^+), we have had success in interpreting[5,18] values of H(25 °C) in terms of a simple geometric model in which water is expelled from the Stern layer by headgroups, counterions, and alkyl groups from the surfactant. Only one adjustable parameter was needed to fit the data at all values of N below the sphere-rod transition employing the *same* parameter for either Na^+ or Li^+. All of the data in Figures 1 and 2 can be reproduced by such a model; however, an additional adjustable parameter describing the change in the number of methyl and methylene groups located in the Stern layer as N or T vary is necessary. The solid lines in Figure 1 are derived from a 2-parameter fit. We do not yet present the details of the model because we do not think that an additional parameter is justified until more corroborating data become available from other techniques.

A very large amount of data were collected in this study, far too much to effectively present in figures or tables. The motive for such extensive data collection was to obtain sufficient statistics in an attempt to distinguish between a model in which α was constant or one in which α increased with an increase in N.[2] Unfortunately, both models fit the data well[2] and a definite conclusion could not be drawn. Nevertheless, these data could be re-interpreted in the future as more is learned about these micelles, thus, the complete data set is presented as Supporting Information.

Microviscosity of Polar Shell. Values of $\tau_{measured}$ were obtained from the line height ratios[13] and microviscosities were computed from eq 7 using eqs 8−10. For TMADS, on average, the ratio τ_B/τ_C departed from unity by 9%, at 10 °C; 4% at 25 °C; and 1% at 45 °C. Thus the reorientation of the nitroxide group in TMADS micelles is approximately isotropic, although slightly less so than in DTAB and DTAC micelles.[10] For the other TAADS micelles, on average, τ_B/τ_C departed from unity by 4% in TEADS at 10 °C, 3% in TBADS at 25 °C, and 2% in TEADS and TPADS at 25 °C. For all other measurements, on average, the departure was 1% or less. Thus, except for TMADS at 10°C, the rotation of the doxyl group of 16DSE in TAADS micelles is very nearly isotropic.

Figure 3a shows the variation of the microviscosity as a function of N for TMADS. The same plot for TEADS at three temperatures (not shown) is very similar to Figure 3. For a given value of N and t, the microviscosity is the same in salt-free and salt-added samples. In Figure 3b representative data for all TAADS micelles at 25 °C are presented. The abscissa for Figure

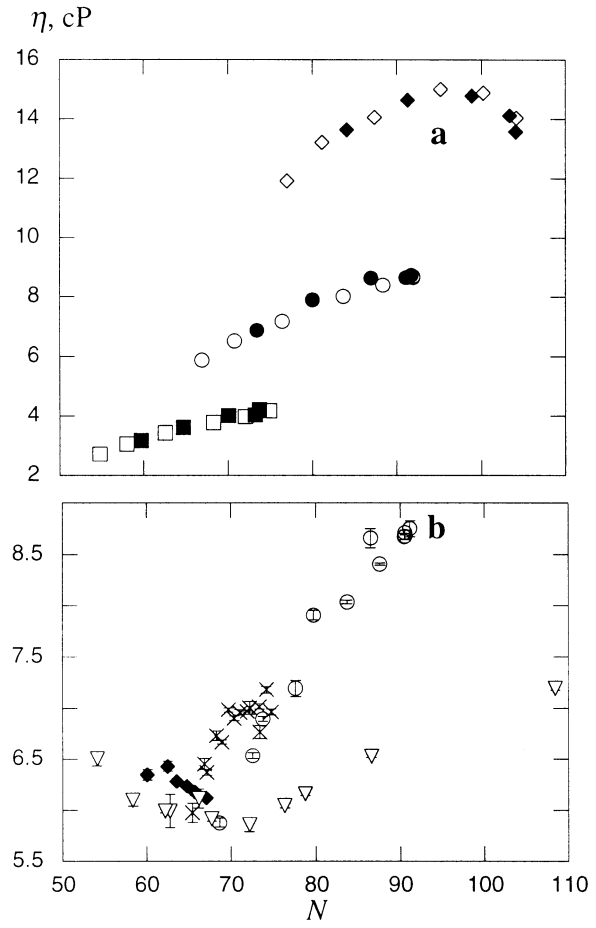

Figure 3. (a) Microviscosity vs the aggregation number for TMADS micelles at 10 °C (◆, ◇), 25 °C (●, ○), and 45 °C (■, □). Open symbols, no added TMACl; closed, added TMACl. (b) Microviscosity vs the aggregation number for TMADS (○), TEADS (×), TPADS (◆), and TBADS (▽) micelles at 25 °C. Data represent both salt-free and salt-added samples. Error bars are standard deviations in 5 measurements.

3 is computed from eqs 3 and 4. As was the case in DTAB, DTAC, and SDS micelles,[10] the microviscosity of the polar shell varies only modestly with N for all TAADS micelles.

Quenching Rate Constants. Figure 4 shows the quenching rate constants[1,3] of pyrene by C_{12}PC as a function of $8RC_QT/3000\eta$ for (a) TMADS and TBADS and (b) TEADS and TPADS. In Figure 4a, the open and closed symbols correspond to results found without and with added salt. C_Q is computed from eq 12 using V_{shell} computed from eq 13. We make the reasonable assumption that the thickness of the polar shell is equal to the diameter of the counterion, $2R_{ci}$ (Table 3). This assumption is a generalization of the principle first stated by Stigter[32] "that, within 1 Å, the thickness equals the length of the hydrated ionic head of the micellized ions." Stigter[32] considered micelles in which the headgroups were large compared with the inorganic counterions and they dominated the dimensions of the Stern layer. Here, we extend the principle using the larger counterions rather than the headgroups to define the thickness. Obviously this is a simplifying assumption to make progress in the absence of data from other experimental methods. Alternatively, the thickness could be modeled to be average of the diameters of the headgroups and the counterions or some other reasonable weighting of these sizes. The predictions of the SES are not very sensitive to minor changes in the thickness and our assumption has the advantage of varying systematically with counterion size. The counterion radii were

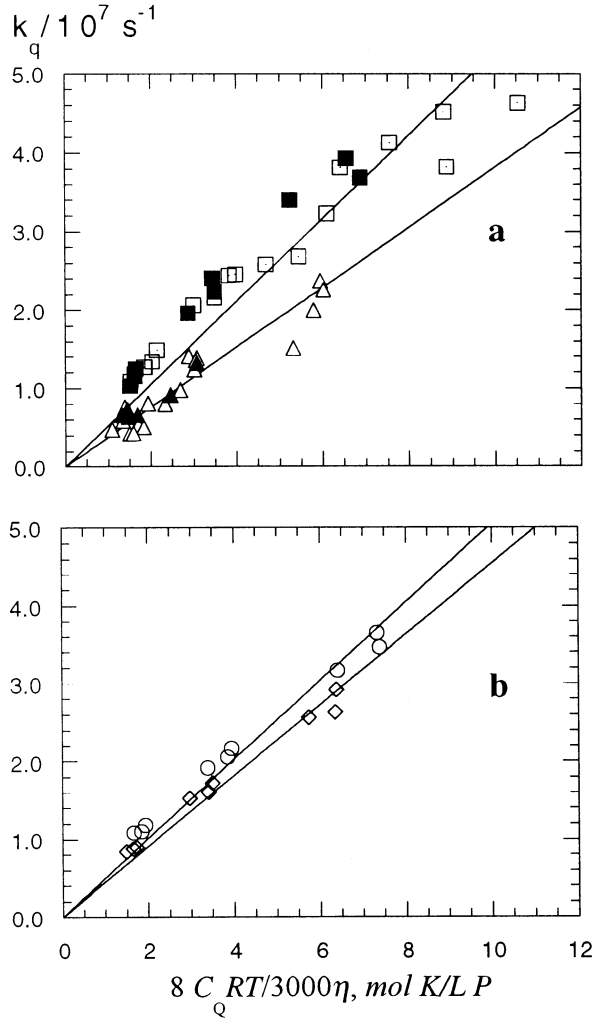

Figure 4. Quenching rate constant of pyrene by C_{12}PC vs the right-hand side of eq 11 with P set equal to unity: (a) TMADS and TBADS; (b) TEADS and TPADS. Symbols are the same as in Figure 2. Data are at 10, 25, and 40 °C taken from refs 1 and 3. The solid lines are eq 11 with P given in Table 3.

TABLE 3: Quenching Probabilities, Zone Displacements δ (Å) and Counterion Diameters

	P	δ, Å	$2R_{ci}$, Å	$\delta/2R_{ci}$
SDS	0.74[a]	0.40	5.0	0.08
TMADS	0.53	0.87	6.4	0.14
TEADS	0.51	1.1	7.8	0.14
TPADS	0.45	1.4	8.8	0.16
TBADS	0.39	1.8	9.6	0.19

[a] Reference 6.

estimated by using Berr's value for the volume of TMA^+ (140 Å^3), adding 4 (26.9 Å^3) for each additional methylene group in the higher members of the TAADS series, and treating the counterions as spheres. The microviscosities are taken from plots such as Figure 3 for t = 10 and 25 °C. For 40 °C, the microviscosities are found by linear interpolation between 25 and 45 °C.The solid lines are the least-squares fit of the data to eq 11 yielding the values of P in Table 3. Also tabulated in Table 3 is the value of P for SDS using C_{16}PC as the quencher taken from the literature.[6]

Discussion

Microviscosity of the Polar Shell. For a given temperature, the microviscosity of the polar shell varies modestly for TAADS

TABLE 4: Microviscosities TAADS Micelles

	t, °C	η, cP
TMADS	10	14. ± 0.8[a]
	25	7.8 ± 1.0[a]
	45	3.7 ± 0.5[a]
TEADS	10	12 ± 0.5[a]
	25	6.5 ± 0.3[a]
	45	3.2 ± 0.1[a]
TPADS	18	8.4[b]
	22	7.0 ± 0.2[c]
	25	6.3[b]
	27	5.9 ± 0.6[c]
	35	4.2[b]
	39	3.6[b]
	43	3.2[b]
	48	2.8[b]
	52	2.5[b]
	56	2.2[b]
	60	2.0[b]
TBADS	10	12 ± 0.6[a]
	25	6.3 ± 0.6[a]
	30	4.5 ± 0.1[a]
	40	3.4 ± 0.04[a]

[a] Mean values and standard deviations over all value of *N*. [b] Standard deviation over 5 spectra <1%. [c] Standard deviation over five spectra.

micelles as the micelles grow. The value of the microviscosity at a given value of *N* is independent of whether that value is produced by adding salt or not. Thus, the microviscosity depends on *N*, and clearly not the micelle concentration. Comparing the 25 °C data in this study, Figure 3b, with Figure 9 of ref 10 shows that the microviscosity and its increase with *N* are remarkably similar in TMADS, TEADS, SDS, and DTAB micelles when compared at the same value of *N*. A small decrease in the microviscosity as a function of *N* is observed for TPADS and TBADS, followed in the latter case with a modest increase. Contrast these results with those found[8] in SDS/nonionic mixed micelles, where a rather large variation of microviscosity was found as the mole fraction of SDS was varied. Averaging the results over all aggregation numbers yields the results in Table 4. One experiment was carried out with [TPADS] = 84.2 mM without salt as a function of temperature. These data are also included in Table 4. A plot of the logarithm of these values versus $1/T$ produces linear plots as shown in Figure 5 adhering to the classical expression of activated viscosity,

$$\eta = \eta_0 e^{E^*/RT} \tag{15}$$

with values of η_0 and E^* given in Table 5. The final row of Table 5 is the result of fitting the results in all TAADS micelles to eq 15, which is the solid line in Figure 5. Compare the values of the activation energies in Table 4 with the similar value of $E^* = 29.1$ kJ/(K mol) found in DTAB micelles[10] and with the value of $E^* = 23.8 \pm 1.2$ kJ/(K mol) averaged over five ethanol/water mixtures from 20 to 60 wt % ethanol. Therefore, with respect to the activation energy of viscosity, the polar shell of TAADS and DTAB micelles are rather normal liquid mixtures, not very different from ethanol−water mixtures.

In part 1,[1] values of E^* were estimated by (1) using the viscosity-sensitive probe 1,3-dipyrenylpropane and (2) from the variation of k_qN with $1/T$. Values of E^* from method 2 were well below those from method 1 and were comparable to those determined here via the spin probe. The detailed variation[1] of E^* with the size of the TAA^+ counterion was slightly larger using method 2 than it is here; however, the average over all of the surfactants, $E^* = 23 \pm 2$ kJ/mol, is similar to that found here, $E^* = 29 \pm 2$ kJ/mol, Table 5. Note that method 2 is essentially a statement of the validity of the temperature dependence expressed by the SES, eq 11.

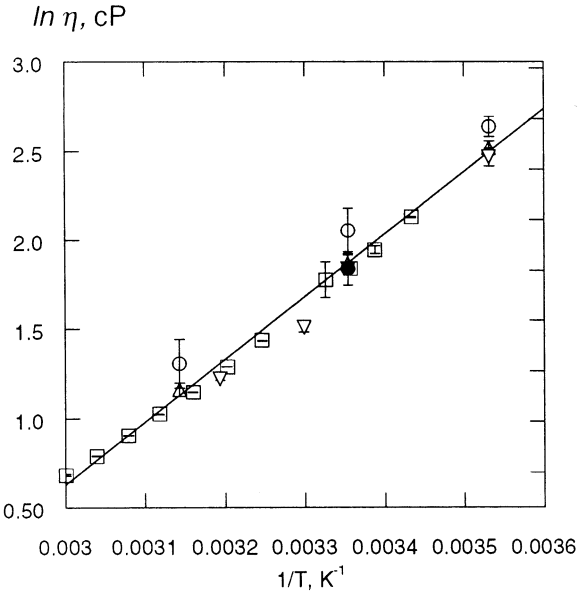

Figure 5. Logarithm of the microviscosity vs the inverse absolute temperature. TMADS (○), TEADS (△), TPADS (□), and TBADS (▽). Values and error bars are the mean values and standard deviations averaged over all aggregation numbers. The value for SDS (●) from the literature.[12] The solid line is the linear least-squares fit to eq 15 for all TAADS; the parameters for this fit and similar fits to each individual surfactant are given in Table 5.

TABLE 5: Activation Energies of the Microviscosities of TAADS. Equation 15

	η_0, cP	E^*, kJ/K mol	*r*
TMADS	7.8×10^{-5}	28.5	.999
TEADS	5.6×10^{-5}	28.9	.999
TPADS	7.7×10^{-5}	28.0	.998
TBADS	2.0×10^{-5}	31.3	.995
All TAADS	4.9×10^{-5}	29.3	.989

Hydrodynamic Description of Bimolecular Collisions in Micelles. First Order Correction to the Zero-Order Model. The linearity of the curves in Figure 4, extrapolating to the origin shows that the SES describes the quenching rate reasonably well in TAADS micelles. A first-order correction to the zero-order model has been proposed[6] to characterize the quite likely fact that the quencher and the fluorophore diffuse through slightly different zones as is schematically suggested in Figure 6. In Figure 6, we suggest that one zone is displaced inward and the other outward from the polar shell each by an amount δ. A portion of the region of diffusive motion of two molecules is shown as two zones, each of which forms a concentric shell about the center of the micelle, only a portion of which is shown for clarity. The purpose of this section is not to suggest that the model of Figure 6 is definitive; rather, we wish to quantify the order of shift necessary to bring experiment and theory into agreement. The results in the section are not changed significantly if we were to suppose, e.g., that zone 1 lies within the polar shell and zone 2 is shifted outward or inward by 2δ. In TAADS micelles, where considerable hydrophobicity is brought to the surface of the micelle by the counterions, it is likely that the average location of pyrene and $C_{12}PC$ would be somewhat different than they would be in SDS.[6] In fact, the pyrene polarity ratio I_1/I_3 shows that pyrene is located in a somewhat more polar environment in TAADS micelles than in SDS.[1]

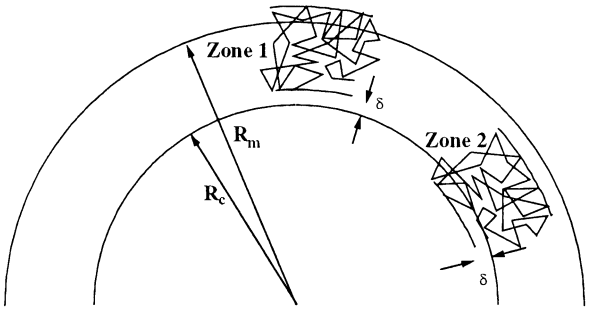

Figure 6. Schematic representation of a first-order correction to the zero-order model. Zones 1 and 2, only a part of which are shown for clarity, extend concentrically around the micelle and represent the volume through which pyrene and $C_{12}PC$ diffuse. These zones are displaced from the Stern layer by equal amounts, δ, one inward and the other outward. The fluorophore and quencher interact quenching the fluorescence only when they collide in the overlap region.

We simplify the model by assuming that each of the molecules 1 and 2 may be found with equal probability at any point within its respective zone of volume V_{zone1} or V_{zone1} and is not found outside those zones. Thus the probability that both molecules will be found in the region of overlap of volume $V_{overlap}$ and thus collide is just

$$P = V^2_{overlap}/V_{zone1}V_{zone2} \tag{16}$$

The suggested configuration of the zones in Figure 6 corresponds to case 2 of the previous work,[6] which yields[6]

$$P = \frac{[(R_m - \delta)^3 - (R_c - \delta)^3]^2}{[(R_m + \delta)^3 - (R_c + \delta)^3][(R_m - \delta)^3 - (R_c - \delta)^3]} \tag{17}$$

In the case of SDS, eq 17 was used to estimate $P = 0.7$, matching the experimental result when $\delta = 0.40$ Å.[6] Values of δ that match the experimental values of P for TAADS are given in Table 3. As might be expected, in view of increasing hydrophobicity and counterion size, the displacements needed to fit the data increase monotonically from Na^+ to TBA^+, growing from $\delta = 0.4$ Å in SDS to $\delta = 1.8$ Å in TBADS. Note that the displacements as a fraction of the shell thickness is similar in all of the TAADS micelles varying from 14 to 20% compared with the 8% observed in SDS. Figure 7 shows all of the data plotted against the RHS of eq 11 using the values of P predicted from eq 17 employing the values of δ in Table 3.

The above simplified treatment assumes that the displacements δ are independent of temperature from 10 to 40 °C to avoid further adjustable parameters. The general conformity of the results to the SES in Figure 7 shows that such variations can be rather small. If this proves to be so in further work, this would tend to support the interpretation of the data in Figure 1 as being due to micelle drying at higher temperatures rather than probe movement with temperature.

Applying case 2, Figure 6, as a first-order correction to the zero-order model shows that reasonable departures from the zero-order model can explain the data. Many other arrangements, including asymmetric displacements, can describe the data and predict similar displacements of about 8−20% of the shell thickness. We observe that employing zone thicknesses that are different from one another would decrease $V_{overlap}$ and thus P.

Note that, for a given temperature, this work and our recent work on DTAB/DATC[10] places the emphasis of the testing of eq 11 on the variation of V_{shell} with N because η varies modestly with N. Contrast this with the results in ref 8 where V_{shell} varied very little and η varied substantially. Both results taken together demonstrate the importance of both V_{shell} and η separately in eq 11.

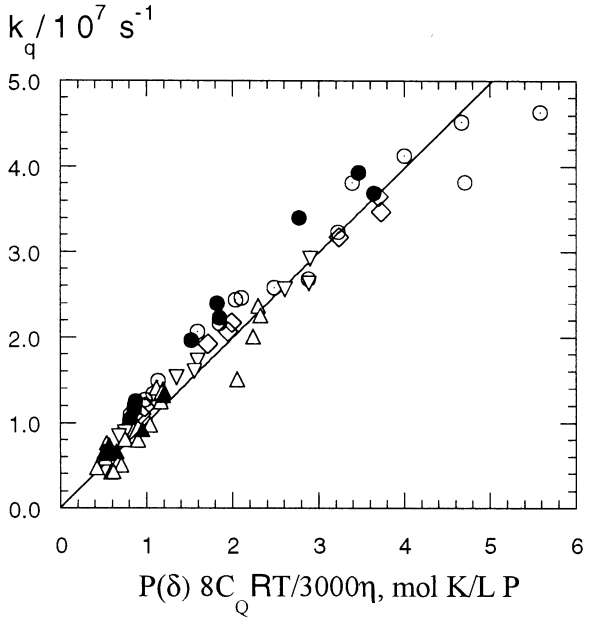

Figure 7. Plot of all quenching rate constants vs the right-hand side of eq 11 with P set equal to values in Table 3, which are predicted from the values of δ given in second column of Table 3. The solid line is eq 11 with $P = 1$. Symbols are the same as in Figure 2.

Hydration of Micelle Surfaces. Figures 1 and 2 show that the hydration of TAADS micelles may be controlled by varying the counterion or the aggregation number, N. Because the hydration does not depend on the particular combination of surfactant and salt concentrations, a given value of $H(t)$ may be maintained as the concentration of micelles is varied in a so-called constant C_{aq} (constant N) experiment.[4,12,33] In particular, extrapolations to zero micelle concentration may be carried out maintaining N and therefore $H(t)$ constant as opposed to traditional extrapolations at constant salt concentrations in which both of these quantities vary.

With the bulky TAA^+ counterions, experiments may be designed using dodecyl sulfate micelles in which rather low levels of water are achieved. Experiments could be designed in which the counterion were varied, but $H(t)$ remained constant; however, these would be limited to values of $H(t)$ of 20% or lower. See Figure 2.

Whether a guest molecule encounters the same volume fraction of water as that shown in Figures 1 and 2 depends on whether it occupies the same average position in the micelle as the spin probe. Obviously, the location of the guest molecule depends on its nature; however, many such molecules can be argued to reside within the polar shell to zero-order. Those molecules might be expected to be displaced somewhat as a function of the counterion, perhaps the aggregation number, and perhaps the temperature; however, these displacements could be reasonably small, as is illustrated by the fact that only small departures are required to bring experiment and theory into agreement for the SES. At a fixed temperature, $H(t)$ decreases upon increasing N, which we have interpreted[5] to be due to a decrease in the available volume to house water in the polar shell. If we tentatively assume that 16DSE does not change average location with temperature, then Figure 1 (and similar results inTEADS) shows that, for a given value of N, TMADS

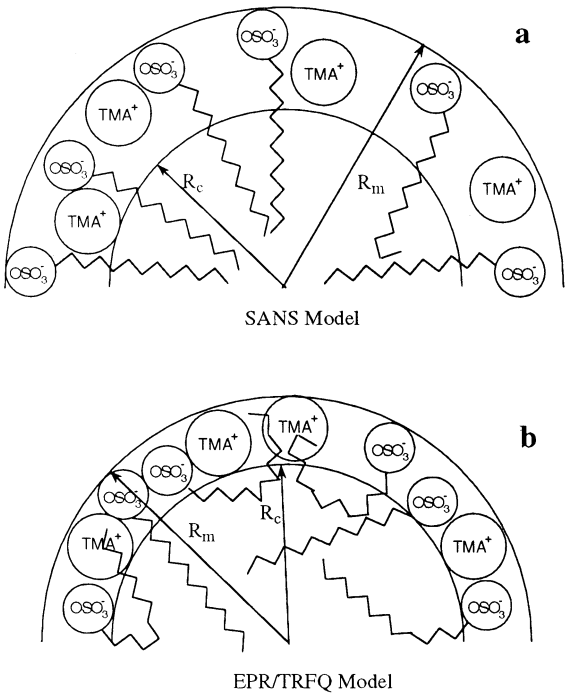

Figure 8. Schematic representation of TMADS micelles (a) proposed by Berr et al.[34] and (b) a proposed model to fit the results in this paper. Only CH_2 groups are "wet" in (a) whereas a few CH_3 groups may also occupy the polar shell in (b). The schematics are to scale for $N \approx 88$ and show approximately the correct amount of alkyl hydrocarbon in the Stern layer.

micelles are dryer at higher temperatures. Figure 1 shows that the variation of $H(t)$ with temperature for a given sample (given values of C and C_{ad}) is minor considering the fact that the change in aggregation number is substantial. The behavior of a given sample is discerned by following the symbols in Figure 1 in approximately a horizontal fashion; dashed lines guide the eye for two such samples. Consider the sample yielding the lower values of $H(t)$. These values vary from about $H(45\ °C) = 0.45$ to $H(10\ °C) = 0.40$ whereas the aggregation number varies from about 65 to 92. At a fixed temperature of 25 °C, this variation in aggregation number would be accompanied by a rather large variation in $H(25\ °C)$ from about 0.60 to 0.33. We offer a tentative model to explain these results that might be amenable to testing. As the micelle grows due to the decreasing temperature, the volume in the polar shell per surfactant molecule decreases. At the same time the amount of alkyl chain hydrocarbon in the polar shell decreases, leaving the volume available for water relatively constant.

Structure of TAADS Micelles. Figure 8a shows a schematic representation of the TMADS micelle as previously advanced by Berr and co-workers on the basis of SANS measurements.[34] The drawing is to scale, corresponding to a value of $N \approx 88$. This corresponds to Berr's results[34] at 30 °C, with [TMADS] = 220 mM, no salt, $N_{wet} = 4.4$ is the number of methlene groups per alkyl chain located in the polar shell, $R_c = 17.2$ Å, and $R_m = 27.5$ Å. An estimate of the hydration of the model in Figure 6a may be obtained by calculating $H(25\ °C) = (V_{shell} - V_{dry})/V_{shell}$, where V_{dry} is the volume inaccessible to water.[5] Using the values in ref 34, this results in $H(25\ °C) = 0.65-0.62$ depending on the value of α employed, $\alpha = 0.34-0.20$, which encompasses the values found by conductivity,[1] SANS,[34] and an aggregation number-based determination.[3] This is considerably larger than the experimental estimate in Figure 1 of $H(25\ °C) = 0.36$. Figure 8b shows a tentative, proposed model that brings the hydration into closer agreement with experiment. Here, the thickness is assumed to be equal to the diameter of the TMA^+ counterion, the same assumption discussed above in connection with the hydrodynamic description of molecular collisions, and envisions that, just as in the SANS model, considerable alkyl chain hydrocarbon occupies the polar shell. In Figure 8b, we have placed an average of an equivalent of $N_{wet} = 3.5$ methylene groups into the polar shell, and set $R_c = 17.5$ Å, and $R_m = 23.9$ Å. In fact, a number of terminal methyl groups are included in the polar shell in Figure 8b, and because these occupy about twice the volume as methylene groups,[29] fewer than 3.5 groups are needed. In Figure 8b, estimating $H(25\ °C)$ from V_{shell} and V_{dry} yields $H(25\ °C) = 0.36$, in agreement with experiment. The schematics are drawn so that approximately the appropriate number of methyl and methylene groups are located in the polar shell. The SANS schematic is modeled after Figure 6 of ref 34 in which a more or less radial configuration of the hydrocarbon tails is depicted.

The SANS schematic, Figure 8a, shows only wet CH_2 groups, because that was the essence of the original model; however, note that to insert a sufficient fraction of hydrocarbon into the polar shell, the average position of the sulfate headgroup is required to be near the outer surface of the polar shell. This results in a nonuniform distribution of the headgroups within the polar shell. In the proposed model, Figure 8b, we have postulated the presence of a significant number of terminal CH_3 groups in the polar shell because this is the most reasonable packing that preserves the dimensions in the model. It is clear that the objection regarding the nonuniform distribution of the sulfate headgroups can easily be resolved in Figure 8a by inserting some methyl groups rather than methylene groups.

The two schematics are very similar except that the value of R_m is significantly larger in the SANS scheme. As a consequence, the volume in the polar shell is larger, leading to larger values of $H(25\ °C)$.

Both models Figure 8a and 8b fill the available volume in the polar shell with water (using a continuum model) but are deduced using different approaches. From SANS, the values of R_c and R_m were found, from which N_{wet} was computed. The number of TMA^+ counterions was computed from the micellar charge, which was taken to be one of the SANS fit parameters. Thus SANS relies on geometric factors to deduce the value of $H(25\ °C)$. In contrast, EPR senses the value of the volume fraction occupied by water and then adjusts the geometry to make the computed value of $H(25\ °C)$ agree with the measured value. Note that there are small discrepancies in the value of N deduced by SANS[19] and TRFQ.[1] These values of N are found using very different approaches; nevertheless, they vary similarly with C_{aq} and their absolute values agree within ±6%. See Figure 5 of ref 2.

Apparently, one way to reconcile the EPR results to the model of Figure 8a would be to suppose that the spin probe spends a significant portion of its time in the core so that the value of $H(25\ °C) = 0$ in the core averaged with the higher value of $H(25\ °C) = 0.65$ would yield the spin-probe sensed value of 0.36. Even if we suppose that the spin probe samples all of the micelle (and none of the surrounding aqueous phase) with equal probability per unit volume, the theoretical average would only be reduced to $H(25\ °C) = 0.49$, still well above the experimental value. Further, allowing the probe to spend a significant amount of time in the core would run counter to a large amount of evidence that most spectroscopic probes, even the rather hydrophobic pyrene, reside near the surface of micelles.[35] In

short, it is difficult to reconcile the measured value of H(25 °C) with the model in Figure 8a.

It is gratifying that the results of SANS,[34] EPR, and TRFQ, not to mention the vast amount of experimental and theoretical work that established[28] the core−shell model long before these latter day methods came along, can be understood in terms of the schematic representations in Figure 8, which differ only in the thickness of the polar shell. It would be interesting indeed to see if the SANS scattering profiles could be fit to the schematic in Figure 8b by some reasonable adjustment of the fitting procedures. In this connection, we note that Griffiths and co-workers[9] have carried out such a program with mixed micelles, using EPR to fix the thickness of the polar shell and then finding a fit to the SANS data.

The hydration of micelles has captured the attention of a very wide spectrum of investigators. A review summarized the situation up to 1980,[35] to which the reader may refer for the already large body of earlier work. That earlier work may be summarized as follows: water associated with the micelle was determined to be that quantity that moved as a kinetic unit with the micelle. Even so, different workers using the same experimental techniques arrived at quite different conclusions as discussed recently.[10]

Only recently have serious attempts to measure $H(t)$ quantitatively in a direct fashion using probes. There have been two very different experimental approaches; chemical trapping of nucleophiles[30] and spin probes.[5,8,10,11] All probe methods must be interpreted with care to ensure that (1) the probe resides where it is postulated to be and (2) the probe is properly sensing the quantity of interest. Implicit in (2) is the assumption that the probe does not modify the hydration of its immediate environment. We have critically addressed these two issues in recent papers and we refer the reader to those assessments.[5,8,10,11]

Other than TMADS, scant data are available for the TAADS micelles. Should these micelles assume a practical importance, presumably more details will emerge from various experimental techniques. On the basis of TRFQ and EPR work on these surfactants plus SANS in the case of TMADS, we offer tentative models of these surfactants that could serve as working hypotheses in further work on the basis of the following assumptions: (1) the core−shell model is generally valid, (2) the thickness of the polar shell is near the diameter of the counterion, (3) a considerable amount of alkyl chain hydrocarbon occupies the polar shell. Item (2) is a generalization of the Stigter[32] principle. Item (3) appears to be required for the predicted values of H(25 °C) be of the order of those in Figure 2. The models, similar to Figure 8b, predict that a significant fraction of the terminal methyl groups be present in the polar shell, a fact that might be verified using NMR together with paramagnetic ions along the lines described by Cabane.[36] To be quatitative, the average location of the paramagnetic ions would have to be determined. This could be possible exploiting the fact that some of these ions, for example Cu^{2+},[37] are effective quenchers of pyrene fluorescence. Carrying out experiments similar to those in Figure 4 and applying a model similar to that in Figure 6 could define the average position of Cu^{2+} relative to pyrene, allowing the relative positions of terminal methyl groups to be defined.

Conclusions

The spin-probe sensed hydration of TAADS micelles, expressed as the volume fraction occupied by water, decreases upon increasing N, which has been understood to be due to a decrease in available volume to house water. $H(t)$ also decreases with the size of the counterion in keeping with the general picture that larger headgroups or counterions expel more water from the polar shell. The microviscosities in TAADS micelles vary modestly with N and in a similar range found for SDS and DTAB. An unexpected result is that the microviscosity in all TAADS micelles is remarkably similar, only TBADS deviates at aggregation numbers above 65. TBADS behaves abnormally at high values of N as has been discussed.[3] The activation energies of the microviscosities of TAADS micelles are very nearly equal to one another and similar to those in SDS and DTAB micelles as well as in ethanol−water mixtures. The only discrepancy in the model of the structure of TMADS micelles derived from SANS results and the present results is the value of the thickness of the polar shell. Guest molecules in TAADS micelles, modeled by the quenching of pyrene fluorescence by C_{12}PC, collide with a rate that is described by the Stokes−Einstein−Smolukhovsky equation varying linearly with T/η passing through the origin with quenching probabilities less than unity. Displacement of the zones through which pyrene and C_{12}PD diffuse by 8% (SDS), 14% (TMADS), 14% (TEADS), 14% (TPADS), and 20% (TEADS) of the polar shell thickness is sufficient to bring all experimental quenching rate constants into agreement with the SES.

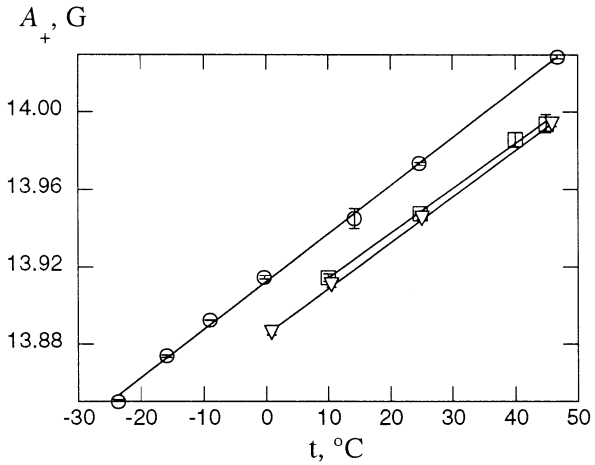

Figure 9. Hyperfine spacing A_+ versus the temperature for 16DSE in three hydrocarbons: *cis*-decalin (○); *n*-decane (□); *n*-hexane (▽). Error bars are standard deviations in five measurements. The solid lines are linear least-squares fit to the data yielding the parameters given in Table 6.

Appendix

Calibration of A_+ versus the Hydrophilicity Index for 16DSE. The variation of A_+ with hydrophilicity index, H(25 °C), valid over the range H(25 °C) = 0.77−0.53 has been published.[11] This range was adequate for SDS,[11] LiDS,[18] and mixtures of SDS with a sugar-based nonionic surfactant.[11] However, as the counterion and/or the headgroup becomes larger in other surfactants, the micelle surfaces become dryer, yielding values of H(25 °C) lower than those of the previous calibration. One purpose of this work was to extend the calibration to lower values of H(25 °C) by employing other solvents and mixtures. However, we find that the differences in the extrapolation of the published calibration and the new results are less than uncertainties in H(25 °C) in micelles, so no change is necessary at 25°. A second purpose is to measure the intrinsic variation of A_+ with temperature so that the method may be used at other temperatures. This variation turns out to be quite small; nevertheless, it is outside of experimental error and is straightforward to investigate.

Figure 9 shows the values of $A_+(t)$ versus the temperature for 16DSE in three hydrocarbons, *cis*-decalin, *n*-octane, and

TABLE 6: Temperature Variation of A_+ for 16DSE in Hydrocarbons

hydrocarbon	A_+(25 °C), G	$(\partial A_+/\partial t)$, mG/K
n-hexane	13.944 ± 0.0006	2.38 ± 0.03
n-decane	13.949 ± 0.0010	2.32 ± 0.07
cis-decalin	13.975 ± 0.0013	2.49 ± 0.04
mean	13.956 ± 0.017	2.40 ± 0.08 mG

n-hexane, which were purchased and used as received from Aldrich. The measurements were identical to those recently detailed.[5] The error bars are the standard deviations in five measurements using the same sample. These uncertainties are somewhat larger than those usually encountered (typically 1−3 mG)[4] in the study of micelles, because spin probe concentrations were maintained below 10 μM to avoid line shifts due to spin exchange.[38] The solid lines are linear least-squares fits yielding the parameters given in Table 6. Because, in hydrocarbons, the value of the hydrophilicity index is strictly zero, the entire variation in $A_+(t)$ is attributed to its explicit temperature dependence $(\partial A_+(t)/\partial t) = 2.40 \pm 0.08$ mG, the mean slope and standard deviation of the three curves in Figure 9. Because we are interested in using the hyperfine spacing to estimate values of the hydrophilicity index, we define the effective hyperfine spacing $A_+^{\text{eff}}(t)$to be the measured value minus the intrinsic variation as follows:

$$A_+^{\text{eff}}(t) = A_+(t) - \left(\frac{\partial A_+}{\partial t}\right)(t - 25°)$$
$$= A_+(t) - 0.0024(t - 25°) \qquad (18)$$

where A_+ is in Gauss when t is in °C.

The EPR of 16DSE was studied in MeOH water mixtures as a function of temperature over the range $t = 0-45$ °C in one set of mixtures and the whole experiment was repeated with another set over the range 10−45 °C. The preparation of the aqueous alcohol mixtures and the details of the measurements have been describe in detail.[5] The temperature was measured to within ±0.2 °C with a thermocouple placed directly into the cavity. Pure methanol was included in each of these series extending the lower limit of H(25 °C) down to 0.438. In addition, measurements were performed in 1,4-dioxane water mixtures at 25 °C.

Finally, we took advantage of the fact that pure TBADS is a liquid above 2 °C to employ it as a solvent to study 16DSE. This adds an interesting dimension to the work because this ionic solvent is formed by large, complicated molecules, more like those comprising the Stern layer of micelles than mixtures of water with small molecules such as methanol and dioxane. Figure 10 shows measurements of A_0, A_+, and A_+^{eff} as a function of temperature. A_0 is one-half the difference in the resonance fields of the high- and low field lines. The fact that $A_0 < A_+$ at temperatures up to 85°C shows that second order shifts due to slow motion effects appreciably affect the value of A_0. See ref 5 and references therein for detailed discussion of the effects of slow motion. It suffices here to recall that A_+ is much less affected than is A_0. Despite the difficulties due to the high viscosity of TBADS, Figure 10 shows that A_+^{eff} is reasonably constant with temperature. Averaging over all temperatures gives $A_+^{\text{eff}} = 14.30 \pm 0.03$ G.

We define the hydrophilicity index to be the molar concentration of OH dipoles in a solution at temperature t, normalized to the OH dipole concentration in water at 25 °C (not at t). This matches Mukerjee's and co-worker's definition[16] at 25 °C and normalizes the index to the density of OH dipoles in water at

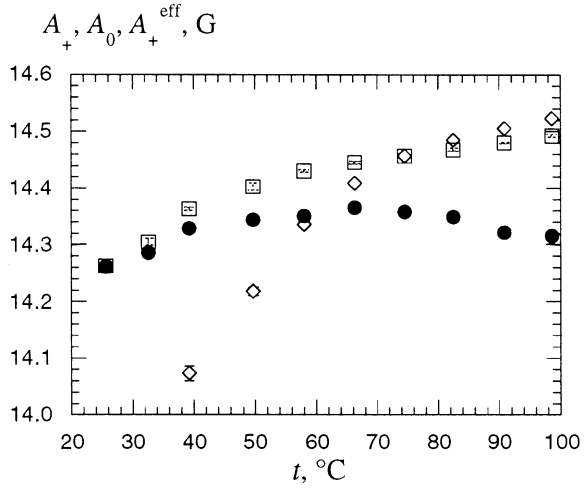

Figure 10. Hyperfine spacings of 16DSE vs temperature for neat TBADS: A_0 (◇); A_+ (□); A_+^{eff} (●). Mean values and standard deviations in 5 measurements.

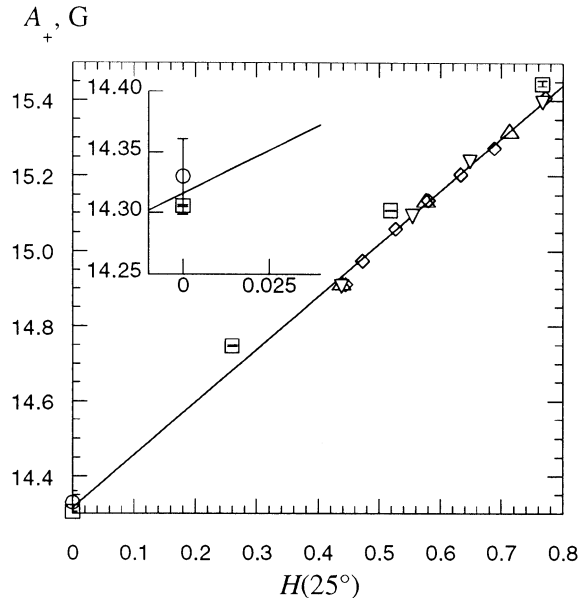

Figure 11. Values of A_+(25 °C) versus H(25 °C) in two new series of MeOH/water mixtures (△ and ▽), a published series of MeOH/water mixtures (◇), dioxane/water mixtures (□), and in neat TBADS (○). The solid line is the previously published[11] calibration given in Table 1. The inset is near the origin. The TBADS datum and error bar is the mean value and standard deviation of A_+^{eff} averaged over all temperatures in Figure 10.

the standard temperature 25 °C. It is straightforward to show that dissolving any compound possessing a single OH bond per molecule in water, will yield the hydrophilicity index $H(x,t)$ given by

$$H(x,t) = \frac{\rho(x,t)}{\rho(0,25\ °C)}\left\{\frac{M_0}{M}x + (1 - x)\right\} \qquad (19)$$

where $\rho(x,t)$ is the density of the solution and x is the weight fraction of the solute of molecular weight M. The density of water at 25 °C and its molecular weight are given by ρ(0,25 °C) and M_0, respectively. For MeOH/H_2O mixtures, eq 19 becomes

$$H(x,t) = \{1.003 - 0.441x)\}\rho(x,t) \qquad (20)$$

Employing experimental values[39] of $\rho(x,t)$ for MeOH/H_2O

mixtures, $H(x,t)$ was computed from eq 20. Dioxane provides no OH dipoles, thus, values of $H(25\ °C) = \rho(1 - x)/\rho_0$ were computed for the dioxane water mixtures using known densities.[40]

Figure 11 shows values of $A_+(25\ °C)$ versus $H(25\ °C)$ for the two runs in MeOH/water mixtures, the dioxane/water mixtures, and the mean value in neat TBADS. The solid line is the published[11] calibration curve. The new data deviate from the previous curve negligibly for the MeOH−water mixtures, the pure dioxane, and the pure TBADS and by an average of + 0.045 G for the dioxane−water mixtures. In view of the assumptions used to interpret values of $H(t)$ in micelles, this latter discrepancy is considered to be within experimental uncertainty.

Plots similar to Figure 11 result at other temperatures. Fitting the MeOH−water mixtures to linear curves yields eq 2 with the constants given in Table 1.

Acknowledgment. We gratefully acknowledge support from NIH/MBRS S06 GM48680-03, the Université Louis Pasteur, and the CNRS. Special thanks are due Philippe Turek and Maxime Bernard for their support with the EPR measurements. We thank Dr. Carolina Vautier-Giongo for the EPR measurements of 16DSE in water−dioxane mixtures.

Supporting Information Available: Mean values and standard deviations of A_+ from five spectra, same sample. This material is available free of charge via the Internet at http://pubs.acs.org.

References and Notes

(1) Benrraou, M.; Bales, B. L.; Zana, R. *J. Phys. Chem. B* **2003**, *107*, 13432.

(2) Bales, B. L.; Tiguida, K.; Zana, R. *J. Phys. Chem. B* **2004**, *108*, 14948.

(3) Zana, R.; Benrraou, M.; Bales, B. L. *J. Phys. Chem. B* **2004**, *108*, 18195.

(4) Bales, B. L. *J. Phys. Chem. B* **2001**, *105*, 6798.

(5) Bales, B. L.; Messina, L.; Vidal, A.; Peric, M.; Nascimento, O. R. *J. Phys. Chem. B* **1998**, *102*, 10347.

(6) Ranganathan, R.; Vautier-Giongo, C.; Bales, B. L. *J. Phys. Chem. B* **2003**, *107*, 10312.

(7) Ranganathan, R.; Peric, M.; Medina, R.; Garcia, U.; Bales, B. L.; Almgren, M. *Langmuir* **2001**, *17*, 6765.

(8) Bales, B. L.; Ranaganathan, R.; Griffiths, P. C. *J. Phys. Chem. B* **2001**, *105*, 7465.

(9) Griffiths, P. C.; Cheung, A. Y. F.; Finney, G. J.; Farley, C.; Pitt, A. R.; Howe, A. M.; King, S. M.; Heenan, R. K.; Bales, B. L. *Langmuir* **2002**, *18*, 1065.

(10) Bales, B. L.; Zana, R. *J. Phys. Chem. B* **2002**, *106*, 1926.

(11) Bales, B. L.; Howe, A. M.; Pitt, A. R.; Roe, J. A.; Griffiths, P. C. *J. Phys. Chem. B* **2000**, *104*, 264.

(12) Bales, B. L. In *Magnetic Resonance in Colloid and Interface Science*; Fraissard, J., Lapina, O., Eds.; Kluwer Academic Publishers: Dordrecht, The Netherlands, 2002; p 277.

(13) Schreier, S.; Polnaszek, C. F.; Smith, I. C. P. *Biochim. Biophys. Acta* **1978**, *515*, 375.

(14) Bales, B. L. In *Biological Magnetic Resonance*; L. J. Berliner, L. J.; Reuben, J., Ed.; Plenum Publishing Corporation: New York, 1989; p 77.

(15) Marsh, D. In *Spin Labeling. Theory and Applications*; Plenum Publishing Corporation: New York, 1989; p 255.

(16) Mukerjee, P.; Ramachandran, C.; Pyter, R. A. *J. Phys. Chem.* **1982**, *86*, 3189.

(17) Schwartz, R. N.; Peric, M.; Smith, S. A.; Bales, B. L. *J. Phys. Chem. B* **1997**, *101*, 8735.

(18) Bales, B. L.; Shahin, A.; Lindblad, C.; Almgren, M. *J. Phys. Chem. B* **2000**, *104*, 256.

(19) Berr, S.; Jones, R. R. M.; Johnson, J. S., Jr. *J. Phys. Chem.* **1992**, *96*, 5611.

(20) Quina, F. H.; Nassar, P. M.; Bonilha, J. B. S.; Bales, B. L. *J. Phys. Chem.* **1995**, *99*, 17028.

(21) Sasaki, T.; Hattori, M.; Sasaki, J.; Nukina, K. *Bull. Chem. Soc. Jpn.* **1975**, *48*, 1397.

(22) Hall, D. G. *J. Chem. Soc., Faraday Trans. 1* **1981**, *77*, 1121.

(23) Jones, L. L.; Schwartz, R. N. *Mol. Phys.* **1981**, *43*, 527.

(24) Wikander, G.; Johansson, L. B.-Å. *Langmuir* **1989**, *5*, 728.

(25) Bales, B. L.; Stenland, C. *J. Phys. Chem.* **1993**, *97*, 3418.

(26) Almgren, M.; Wang, K.; Asakawa, T. *Langmuir* **1997**, *13*, 4535.

(27) Ranganathan, R.; Okano, L. T.; Yihwa, C.; Alonso, E. O.; Quina, F. H. *J. Phys. Chem. B* **1999**, *103*, 1977.

(28) Hartley, G. S. *Aqueous Solutions of Paraffin-Chain Salts*; Hermann and Cie: Paris, 1936.

(29) Tanford, C. *The Hydrophobic Effect: Formation of Micelles and Biological Membranes*; Wiley-Interscience: New York, 1980.

(30) Soldi, V.; Keiper, J.; Romsted, L. S.; Cuccovia, I. M.; Chaimovich, H. *Langmuir* **2000**, *16*, 59.

(31) Marsh, D. *J. Magn. Reson.* **2002**, *157*, 114.

(32) Stigter, D. *J. Phys. Chem.* **1964**, *68*, 3603.

(33) Griffiths, P. C.; Paul, A.; Heenan, R. K.; Penfold, J.; Ranganathan, R.; Bales, B. L. *J. Phys. Chem. B.* **2004**, *108*, 3810.

(34) Berr, S. S.; Coleman, M. J.; Jones, R. R. M.; Johnson, J. S., Jr. *J. Phys. Chem.* **1986**, *90*, 6492.

(35) Lindman, B.; Wennerström, H.; Gustavsson, H.; Kamenka, N.; Brun, B. *Pure Appl. Chem.* **1980**, *52*, 1307.

(36) Cabane, B. *J. Phys.* **1981**, *42*, 847.

(37) Bales, B. L.; Almgren, M. *J. Phys. Chem.* **1995**, *99*, 15153.

(38) Bales, B. L.; Peric, M. *J. Phys. Chem. A* **2002**, *106*, 4846.

(39) Mellan, I. *Industrial Solvents Handbook*; Noyes: Park Ridge, N. J., 1970.

(40) Timmermans, J. *The Physicochemical Constants of Binary Systems in Concentrated Solutions*; Interscience: New York, 1960.